science, engineering and health studies

Research Article

Science, Engineering and Health Studies
https://li01.tci-thaijo.org/index.php/sehs
ISSN (Online): 2630-0087

Design and manufacture of gelatin-alginate scaffolds for tissue engineering based on three-dimensional extrusion bioprinting

Dung Quoc Nguyen[1,3], Nghia Thi Hieu Phan[1,2,3], My Thi Ngoc Nguyen[1,2,3], and Ha Le Bao Tran[1,2,3]*

[1] Department of Physiology and Animal Biotechnology, Faculty of Biology and Biotechnology, University of Science, Ho Chi Minh City, Vietnam
[2] Laboratory of Tissue Engineering and Biomedical Materials, University of Science, Ho Chi Minh City, Vietnam
[3] Vietnam National University, Ho Chi Minh City, Vietnam

***Corresponding author**:
Ha Le Bao Tran
tlbha@hcmus.edu.vn

***Received**: 20 February 2023*
***Revised**: 13 October 2023*
***Accepted**: 17 October 2023*
***Published**: 28 December 2023*

***Citation**:
Nguyen, D. Q., Phan, N. T. H., Nguyen, M. T. N., and Tran, H. L. B. (2023). Design and manufacture of gelatin-alginate scaffolds for tissue engineering based on three-dimensional extrusion bioprinting. Science, Engineering and Health Studies, 17, 23050014.

ABSTRACT

Scaffolds play an important role in tissue engineering, serving as the structural framework for different biological processes, including cell proliferation, tissue creation, and organ regeneration. Adding calcium chloride ($CaCl_2$) as a pre-crosslinking agent to the ink used in three-dimensional (3D) bioprinting can change the properties of the scaffold. In this study, we engineered scaffolds using ink comprising 10% gelatin, 10% alginate, and varying concentrations of $CaCl_2$, utilizing 3D extrusion bioprinting technology. Three distinct scaffolds, named F1, F2, and F3, were created using different concentrations of $CaCl_2$: 60 mM for F1, 70 mM for $CaCl_2$, and 80 mM for F3. After fabrication, they underwent crosslinking with 100 mM of F2 to enhance their stiffness. The 3D printed scaffolds were evaluated based on four tests: mechanical testing, FTIR analysis, *in vitro* cytotoxicity, and cell viability. The results demonstrated that the crosslinked scaffolds exhibited significantly greater stiffness, compared to their uncrosslinked counterparts, with F3 exhibiting the highest stiffness. The Fourier-transform infrared spectroscopy (FTIR) results indicated the presence of characteristic peaks for gelatin (N-H, C=O) and alginate (O-H, COO^-, and C-O-C) in F1, F2, and F3 scaffolds, along with a slight leftward shift in absorbance peaks. This suggests an interaction between alginate and $CaCl_2$. Importantly, all the scaffolds exhibited non-cytotoxicity properties. However, the relative growth rate (RGR) in F3 was significantly lower than that in F1 and F2, attributable to the higher concentration of $CaCl_2$ used in its preparation. Furthermore, promising cell viability was observed within all the scaffolds that were 3D printed using cell-laden bioinks. This observation was made 24 h after the printing process when the printed scaffolds were returned to their culture conditions. This research contributes to the foundational development of 3D printed scaffolds and their potential applications in advancing tissue engineering research.

Keywords: 3D bioprinting; alginate; cell-laden bioink; crosslink; gelatin; scaffolds

1. INTRODUCTION

Scaffolds play a crucial role in tissue engineering by providing constructs that mimic the natural microenvironment of cells, influencing cell growth, cell proliferation, tissue creation, and organ regeneration. Scaffolds have recently emerged as an alternative solution for repairing, replacing, and regenerating damaged tissues caused by trauma, sickness, or congenital disorders, aiming to improve or increase their functionality (Benwood et al., 2021; Vitus et al., 2021). Scaffolds can be generated using a variety of methods. Among these, 3D bioprinting is a commonly utilized approach in tissue engineering to fabricate scaffolds due to its capacity to manufacture a large number of products with the same geometric shape in a short amount of time, In addition, it allows tunable hole size, porosity, and cell distribution in the scaffolds (An et al., 2015; Benwood et al., 2021). In 3D bioprinting-based extrusion, the material is extruded to form a filament, which is stacked to produce a product with a shape based on a 3D model developed by computer-aided design (CAD) (Benwood et al., 2021; Gopinathan and Noh, 2018). Inks are the materials utilized in printing processes to create various printed products, and they include three major groups: metals, ceramics, and polymers. Alginate and gelatin are promising biomaterials used in making inks for 3D bioprinting applications (Alizadeh-Osgouei et al., 2019; Giuseppe et al., 2018; Rottensteiner et al., 2014).

Alginate is commonly used in various biomedical applications, including wound healing, medication administration, and tissue engineering. This is due to its biocompatibility and ability to create hydrogels that mimic the characteristics of the extracellular matrix of tissues and are not degraded by enzymes produced by mammals (Benwood et al., 2021; Gopinathan and Noh, 2018). However, alginate does not contain cell adhesion sites. To address this limitation, alginate can be combined with gelatin. Gelatin, a natural polymer produced by the partial hydrolysis of collagen, is a common ingredient in bioink. It is used in the formulation of bioinks for 3D printing due to its biocompatibility and biodegradability features (Benwood et al., 2021; Giuseppe et al., 2018; Roi et al., 2019). In addition, it has Arg-Gly-Asp (RGD) sites for cell adhesion, which facilitate attachment, growth, and multiplication of cells to produce their extracellular components and form tissues (Benwood et al., 2021; Datta et al., 2020; Ramiah et al., 2020; Rottensteiner et al., 2014; Unagolla and Jayasuriya, 2020). Gelatin can form hydrogel at temperatures below 25 °C due to the formation of triple helices and a rigid 3D network. This property allows gelatin to be printed and stacked on itself in a controlled manner. However, the conformation switches from a helix to a more flexible coil at temperatures above 30 °C, reverting the gel to a liquid state (Klouda and Mikos, 2008; Tan et al., 2020). This causes gelatin to melt, rendering it unable to hold or retain its structure at a physiological temperature (Tan et al., 2020).

Based on their respective advantages, we combined gelatin and alginate in this work to create scaffolds. However, the resulting scaffolds were unstable and underwent rapid biodegradation. $CaCl_2$ can be used as a crosslinking agent to improve the printability of the bioink and enhance the stiffness of the scaffolds (GhavamiNejad et al., 2020; Nelson et al., 2021). Hence, after printing the scaffolds, we applied a 100-mM $CaCl_2$ solution as a crosslinking agent to strengthen the stability of their structure. Adding $CaCl_2$ as a pre-crosslinking agent to the ink can change the properties of scaffolds. A challenging issue is that ionic crosslinkers may impact cell damage and survival during and after the 3D bioprinting process. Previous research has shown that the concentration and exposure duration of ionic crosslinkers affected the viability and proliferative capability of cells in alginate-based hydrogels. Furthermore, it has been reported that increased levels of Ca^{2+} are hazardous to cells inside the 3D bioprinted structure (GhavamiNejad et al., 2020). Therefore, in this study, we designed and fabricated 3D-printed scaffolds using a combination of gelatin (10%), alginate (10%), and $CaCl_2$ as pre- and post-crosslinking agents. The 3D-printed scaffolds were assessed based on four tests: mechanical testing, FTIR analysis, *in vitro* cytotoxicity, and cell viability.

2. MATERIALS AND METHODS

2.1 Materials

Alginic acid, sodium salt, isolated from brown algae (batch no. MKCJ8027, BioReagent), gelatin from bovine skin (type B, batch no. SLCC6365, BioReagent), Dulbecco's Modified Eagle Medium F12 (DMEM/F12, batch no. RNBJ7249, BioReagent), fetal bovine serum (FBS, batch no. BCCC8749), and penicillin/streptomycin (batch no. 049M4858V, BioReagent) were procured from Sigma Aldrich (St. Louis, USA). $CaCl_2$ powder (batch no. 1023780500, Reag. Ph Eur) and ethanol (batch no. 1009831000, ACS, ISO, Reag. Ph Eur) were acquired from Merck (Darmstadt, Germany). Phosphate-buffered saline pH 7.4 (PBS, batch no. 2492797) was purchased from Gibco (Carlsbad, USA). Crystal violet (batch no. 061M18522V, BioReagent), dimethyl sulfoxide (DMSO, batch no. STBF8663V) and 3-[4,5-dimethylthiazol-2-yl]-2,5 diphenyl tetrazolium bromide (MTT, batch no. MKBQ9338V, BioReagent) were purchased from Gibco (Carlsbad, USA). The human fibroblast cells used in this study were provided by the Laboratory of Tissue Engineering and Biomedical Materials at the University of Science in Ho Chi Minh City, Vietnam.

2.2 3D model design

The 3D model was designed using Solidworks CAD software (Dassault Systemes Solidworks Corporation, USA) integrated with the software of a 3D printer (Bio X™, Cellink, Gothenburg, Sweden). The dimensions of the 3D model are 20 mm (length) x 20 mm (width) x 0.5 mm (height) (Figure 1A). The structure is divided into two layers, each with a height of 0.25 mm. The ink lines inside the structure were filled 10% with grid lines (Figure 1B).

2.3 Preparation of inks

Sodium alginate powders, gelatin powders, and $CaCl_2$ powders were dissolved in deionized water. The gelatin-alginate ink was prepared by mixing 10% w/v of gelatin, 10% w/v of alginate, and $CaCl_2$ solution in a volume ratio of 1:1:1. The concentration of $CaCl_2$ was 60 mM, 70 mM, and 80 mM, for the generated inks F1 (gelatin 10%, alginate 10%, $CaCl_2$ 60 mM), F2 (gelatin 10%, alginate 10%, $CaCl_2$ 70 mM), and F3 (gelatin 10%, alginate 10%, $CaCl_2$ 80 mM). These inks were transferred into 3 mL syringes, and the bubbles in the inks were removed by centrifugation at 3000 rpm for 2 min. The inks were then stored at 4 ˚C until use.

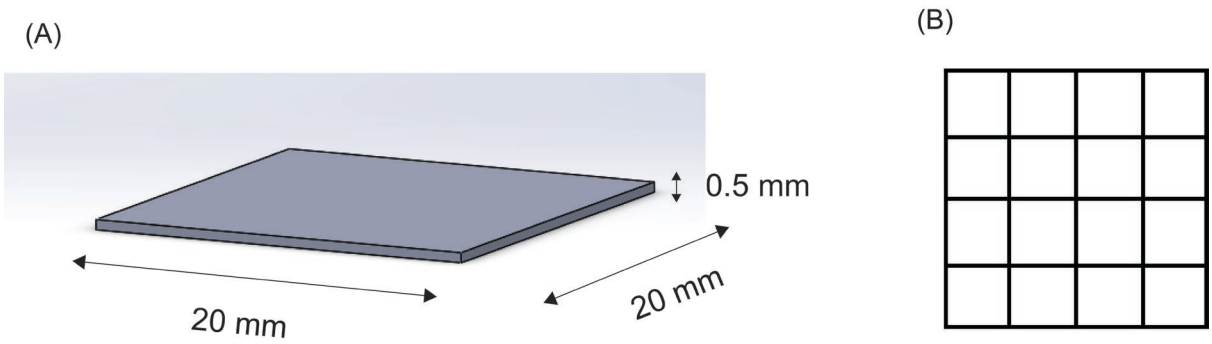

Figure 1. Orientation of the 3D model as scaffolds, showcasing (A) 3D Solidworks models, and (B) grid line pattern

2.4 Fabrication of 3D printed scaffolds

The gelatin-alginate inks were loaded into the printer machine, and the printing process was performed on the bioprinting platform (Bio X™ 3D Bioprinter, Cellink, Gothenburg, Sweden), equipped with a syringe pump printhead and a 25G print nozzle (Cellink, Gothenburg, Sweden). The scaffolds were printed using the following printing parameters: a volume/distance ratio of 0.5 µL/mm, a print speed of 15 mm/s and an infill density of 10%. To improve the stability, the printed scaffolds were crosslinked with a 100 mM $CaCl_2$ solution and then washed three times with 1X PBS solution to remove $CaCl_2$ residue.

2.5 Characterization of 3D printed scaffolds

2.5.1 Mechanical test

The stiffness of the scaffolds was assessed by the ability to withstand mechanical forces. The scaffolds were determined to withstand maximum mechanical compression using a CT3 Texture Analyzer (CT3-100, Brookfield, MA, United States). Mechanical force (N) was applied to each scaffold at five different positions, and the forces required to break the structure were recorded.

2.5.2 FTIR analysis

The chemical bonds of F1, F2, and F3 scaffolds were determined by the FTIR spectrometer (Perkin Elmer Frontier FTIR, PerkinElmer, Shelton, USA). The samples were measured in pelletizing KBr conditions with a wave number range of 4000–400 cm^{-1}.

2.5.3 *In vitro* cytotoxicity

In vitro cytotoxicity was evaluated using both direct contact tests and tests on extracts following the ISO 10993-5 standard (Thangaraju and Varthya, 2022). The culture medium was utilized as a negative control, latex gloves were employed as a positive control, and F1, F2, and F3 scaffolds were used as testing samples. The culture medium was DMEM/F12 supplemented with 10% FBS and 1% penicillin/streptomycin.

Test by direct contact

Human fibroblast cells were seeded into 4-well plates at a density of $5x10^4$ cells/well, and they were then incubated with 5% CO_2 at 37 °C for 24 h. The old medium was replaced with 500 µL fresh medium. The F1, F2, and F3 scaffolds were put on the cell surface, and the area of the scaffolds was not more than 10 percent, compared with each well plate area. After that, these plates were incubated with 5% CO_2 at 37 °C for 24 h. The cells were stained with a 0.6% crystal violet solution for 30 min, after which the solution was removed, and the cell rinsed with 1X PBS. An inverted microscope (Olympus CKX53, Olympus, Tokyo, Japan) was used to observe and assess the morphology of the cells.

Test on extracts

To get extracts following the ISO 10993-12 standard, F1, F2, and F3 scaffolds were immersed in cell culture media at a rate of 3 cm^2/mL (total surface area of scaffolds/volume of cell culture media) for 24 h (Thangaraju and Varthya, 2022). At a density of 10^4 cells per well, the fibroblasts were seeded into 96-well plates and cultivated with 5% CO_2 at 37 °C. When the cell density reached about 80% confluency, the old medium was removed, and 100 µL of F1, F2, or F3 extracts were added. Then, the plates were incubated with 5% CO_2 at 37 °C. After 24 h, the extracts were replaced with 100 µL of MTT solution (0.5 mg/mL), and the cells were incubated at 37 °C for 4 h (protected from light). After that, the MTT solution was removed. Then, 100 µL of DMSO/ethanol (1:1 v/v) was added and gently mixed. The degree of cytotoxicity was determined by measuring absorbance at 570 nm in the microplate reader (EZ Read 400, Biochrom Ltd., Cambridge, UK). The relative growth rate (RGR, %) was calculated using Equation (1) below:

$$The\ relative\ growth\ rate\ (RGR)\ \% = \frac{Absorbance\ of\ treated\ wells}{Absorbance\ of\ negative\ control} \times 100 \quad (1)$$

2.5.4 Cell viability

Using the MTT method, cell viability on the scaffolds was evaluated. In this experiment, the experimental groups included a negative control (containing only the culture medium), a positive control (human fibroblast cells in the culture medium), and three experimental samples (F1, F2, and F3 scaffolds made from cell-laden bioinks).

To make cell-laden bioinks, human fibroblast cells (10^7 cells) were mixed with 1 mL each of F1, F2, and F3 ink using the Cellmixer device (Cellink, Gothenburg, Sweden). These cell-laden bioinks were used by the 3D printer to produce the F1, F2, and F3 cell-laden scaffolds. The scaffolds were then crosslinked with a 100-mM $CaCl_2$ solution and washed three times in the cell medium.

The scaffolds were incubated with 5% CO_2 at 37 °C. After 24 h, 100 µL of MTT solution (0.5 mg/mL) was added and then it was incubated with 5% CO_2 at 37 °C for 4 h. The formazan crystal was examined using an inverted microscope (CKX53, Olympus, Tokyo, Japan).

2.6 Statistical analysis

Each experiment was repeated three times. The one-way ANOVA (analysis of variance) test was used in the statistical study to identify significant difference. Statistical significance was defined as $p<0.05$.

3. RESULTS

3.1 Fabrication of printed scaffolds

These scaffolds were created by 3D printing using F1, F2, and F3 inks. The shapes are seen in Figure 2.

We added methylene blue stain to facilitate visibility. The structure of the obtained scaffolds was a grid pattern. The size of the scaffolds was about 20 x 20 mm. We also immersed these scaffolds into 100 mM $CaCl_2$ solution to increase their stiffness. It was observed that the scaffold colors were opalescent after they were crosslinked, while the scaffolds not crosslinked were translucent (Figure 3).

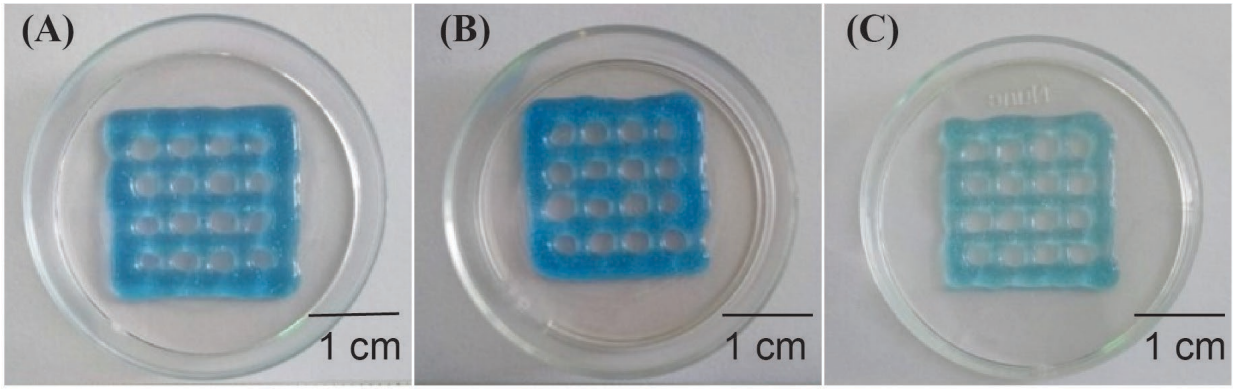

Figure 2. The images of the scaffolds; (A) F1 scaffold, (B) F2 scaffold, (C) F3 scaffold

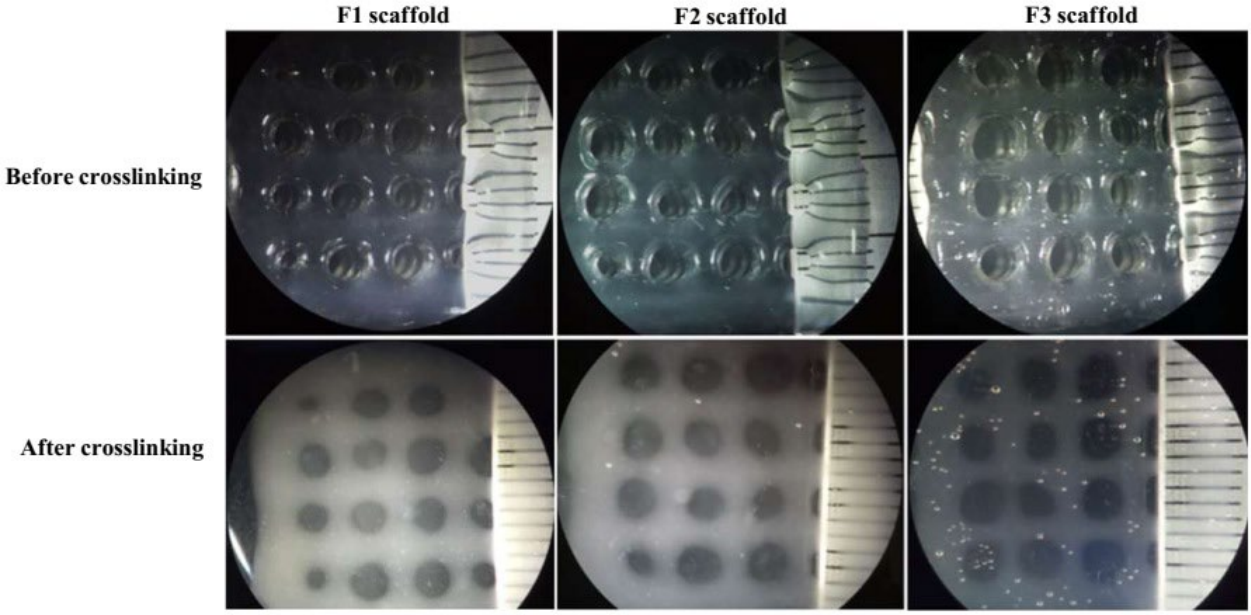

Figure 3. F1, F2, and F3 scaffolds before and after crosslinking with 100 mM $CaCl_2$ solution

3.2 Evaluation of printed scaffolds

3.2.1 Mechanical test

The stiffness of F1, F2, and F3 scaffolds is expressed through their ability to withstand mechanical compressive forces on the structure. The minimum compressive force required to break the structure was determined using a CT3 Texture Analyzer. The results are shown in Figure 4.

The crosslinked F1, F2, and F3 scaffolds exhibited higher resistance to compressive forces than the uncrosslinked F1, F2, and F3 scaffolds. In particular, the least compressive force needed to break the uncrosslinked F1, F2, and F3 scaffolds was 0.63±0.22 N, 2.01±0.53 N, and 4.64±0.63 N, respectively. After crosslinking, the minimum compressive force needed to

break each of the scaffolds increased to 3.73±0.48 N, 4.27±0.52 N, and 6.07±0.77 N, respectively. This enhancement in the ability of the scaffolds to withstand mechanical impact after crosslinking highlights the increased stiffness of the crosslinked F1, F2, and F3 scaffolds, compared to their uncrosslinked counterparts

The crosslinked F3 had the highest capacity to withstand the impact of compression force and was substantially different from the crosslinked F1 and F2 scaffolds (p<0.05). In conclusion, the crosslinking process made the scaffolds to be much more rigid. Among the three crosslinked scaffolds (F1, F2, and F3), the crosslinked F3 scaffold exhibited the highest stiffness, capable of withstanding compression stresses of 6.07 N.

3.3 FTIR analysis

FTIR spectra confirmed the chemical functional groups of gelatin, alginate, and the F1, F2, and F3 printed scaffolds (Figure 5).

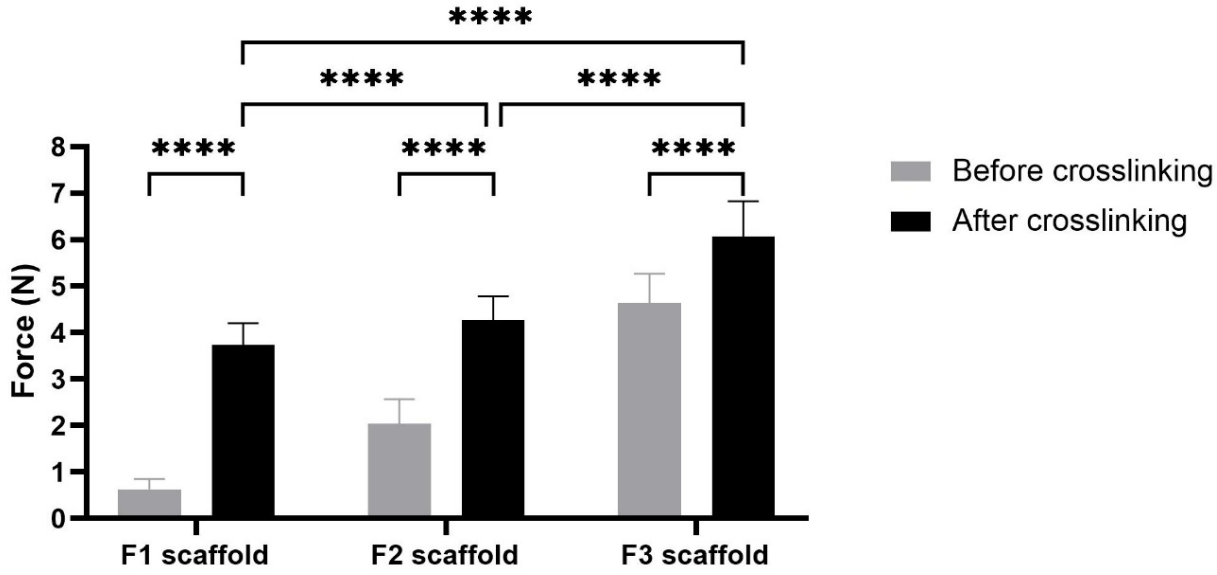

Figure 4. The stiffness of F1, F2, and F3 scaffolds before and after crosslinking
Note: Asterisks (****) indicate statistical significance (p<0.0001)

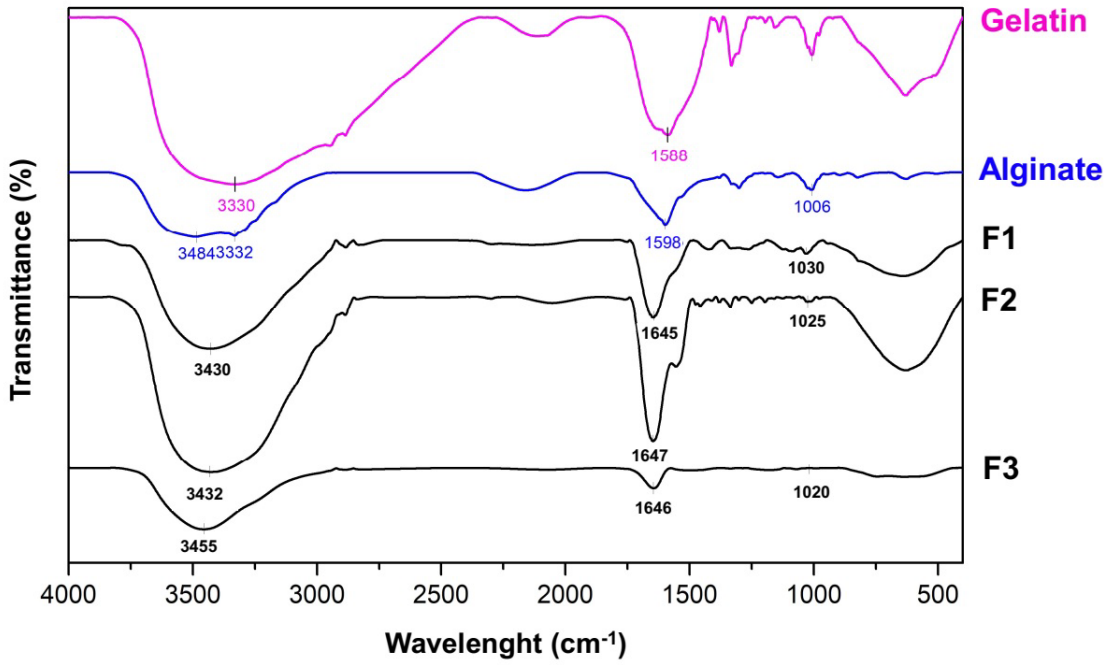

Figure 5. FTIR spectra of gelatin, alginate, F1, F2, and F3 scaffolds

The characteristic peaks of gelatin were observed at 3330 cm^{-1} (N-H bond, amide A group) and 1588 cm^{-1} (C=O bond, amide I group). The characteristic peaks of alginate were identified at 3484–3332 cm^{-1} (O-H), 1598 cm^{-1} (COO^-, carboxylate salt ion), and 1006 cm^{-1} (C-O-C) (Fernandes et al., 2018; Pan et al., 2016). There were N-H, C=O, O-H, and C-O-C bonds found in samples of F1, F2, and F3 scaffolds. However, there was a small shift to the left in the absorbance peaks of the crosslinked samples. It was seen that the amide I peak (1588 cm^{-1}) and carboxylate salt ion peak (1598 cm^{-1}) shifted to 1647 cm^{-1} for F1 scaffolds, 1647 cm^{-1} for F2 scaffolds, and 1646 cm^{-1} for F3 scaffolds in the spectrum. These shifts may indicate the impact of crosslinking between alginate and $CaCl_2$ (Daemi and Barikani, 2012; Haider et al., 2020).

3.4 *In vitro* cytotoxicity

Figure 6 shows the results of the cytotoxic assessment in the direct contact test. The cells treated with F1, F2, and F3 scaffold samples showed typical human fibroblast shapes, even in the areas where they had direct contact with the scaffolds. Also, this observation was consistent with the control (Figures 6A, 6C, 6D, and 6E).

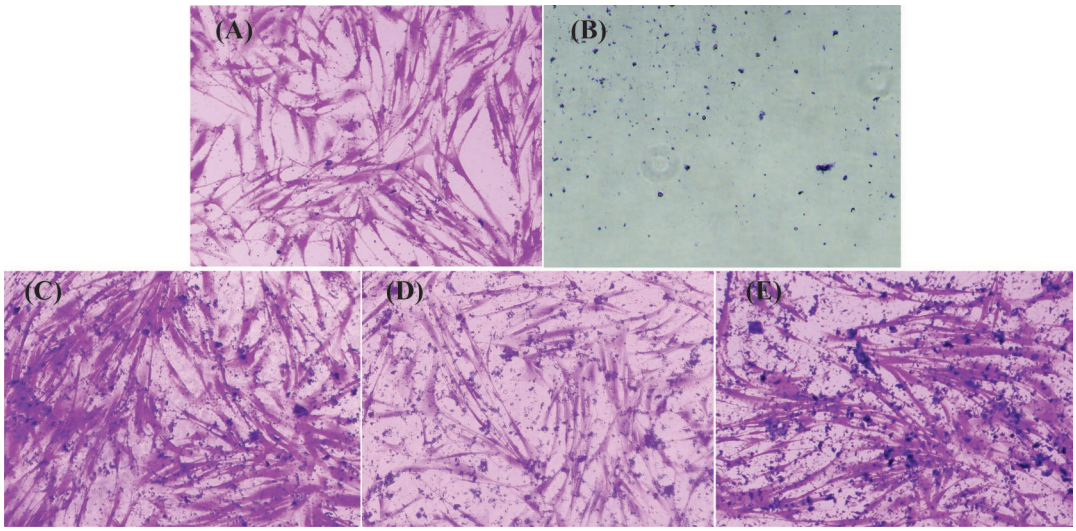

Figure 6. Morphology of human fibroblast cells following crystal violet staining in direct contact test; (A) culture medium, (B) latex, (C) F1 scaffold, (D) F2 scaffold, (E) F3 scaffold

F1, F2, and F3 scaffold groups showed some cellular deterioration and mortality indications. Therefore, the MTT assay was employed for the cytotoxic test on the extracts to verify the cytotoxicity of F1, F2, and F3 scaffolds (Figure 7). According to ISO 10993-5, the substance was regarded as non-cytotoxic for tests on the extracts if the RGR was ≥70% (Thangaraju and Varthya, 2022). The RGR of cells after treatment with F1, F2, and F3 extracts were 99.42%±7.53, 90.36%±2.75, and 80.66%±1.14, respectively, which were all higher than 70%. These findings demonstrated that F1, F2, and F3 scaffolds are not cytotoxic.

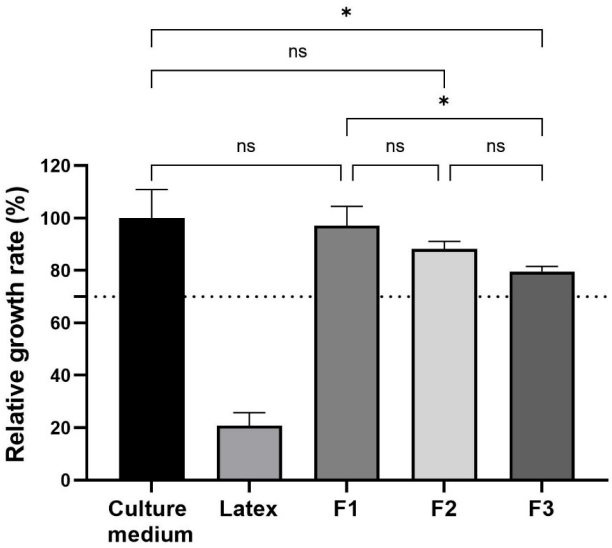

Figure 7. The relative growth rate of cells in tests on extracts
Note: Asterisks (*) indicate statistical significance (p<0.05), and 'ns' denotes nonsignificant results.

3.5 Cell viability

Cell viability was determined by the MTT method based on the appearance of purple MTT-formazan crystals. Figure 8 shows that formazan crystals were formed in the cells treated with extracts of F1, F2, and F3 scaffolds. It was obvious that MTT-tetrazolium salt (yellow) was converted into insoluble crystals of MTT-formazan (purple) by the enzyme mitochondrial dehydrogenase. This result showed the viability of the cell after being incubated with extracts of F1, F2, and F3 scaffolds for 24 h.

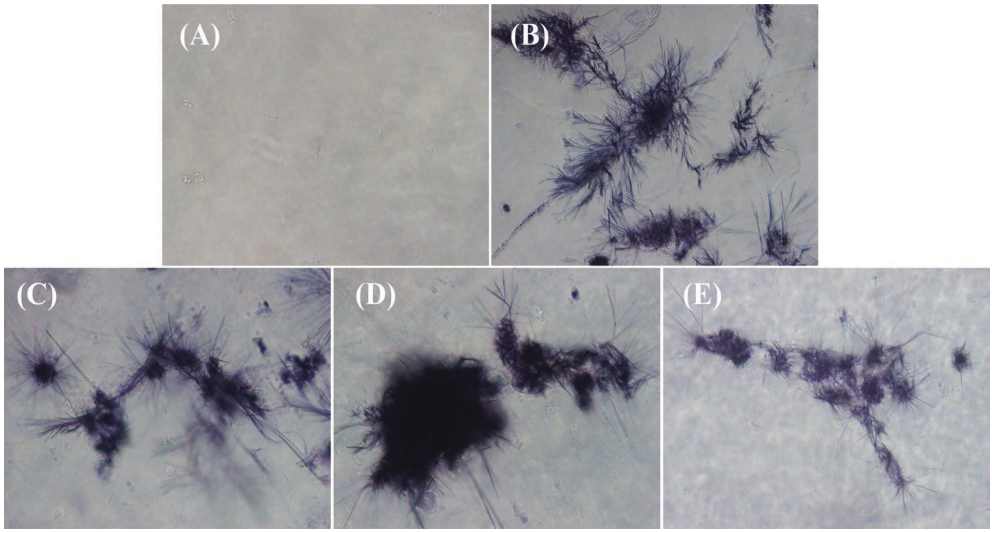

Figure 8. Formazan crystal in the cells after incubation with extracts from F1, F2, and F3 scaffolds (at 40x magnification); (A) cell culture medium, (B) fibroblast cells in cell culture medium, (C) the cells treated with extract of F1 scaffold, (D) the cells treated with extract of F2 scaffold, and (E) the cells treated with extract of F3 scaffold

4. DISCUSSION

In this study, we used 3D bioprinting technology to create scaffolds made of gelatin, alginate, and varying concentrations of $CaCl_2$. Gelatin and alginate are natural polymers with outstanding biocompatibility, gel-forming ability, non-toxicity, biodegradability, and ease of processing, making them suitable for the fabrication of scaffolds (Afewerki et al., 2019; Sahoo and Biswal, 2021). We employed a two-step crosslinking process using $CaCl_2$: (1) in the ink formula at concentrations of 60 mM, 70 mM, and 80 mM to form gel states suited for the printing process; (2) after printing the structure, at concentrations of 100 mM to increase the stability of the scaffolds. The results demonstrated that crosslinking the printed scaffolds in a 100-mM $CaCl_2$ solution significantly increased their ability to withstand mechanical compression. Each Ca^{2+} can form coordination bonds with two G units of the molecular alginate chain, forming the "egg-box" structure and enhancing the structure's stiffness (Zhang et al., 2022). Compared to the other two scaffolds, the crosslinked F3 scaffold showed the highest ability to withstand compressive strength. This can be explained by the difference in the concentration of $CaCl_2$ added to the printing ink formulation. Out of the three scaffolds, the F3 scaffold contained the highest concentration of $CaCl_2$. This also suggests that increasing the concentration of $CaCl_2$ might improve the structure's rigidity. However, high concentrations of Ca^{2+} residue might harm cells in scaffolds, so we evaluated the cytotoxicity property *in vitro*. Previous research has shown that the viability and growth of cells in an alginate-based hydrogel were affected by the concentration and time of the ionic crosslinker. Excess Ca^{2+} may also be hazardous to 3D bioprinted cells. High concentrations of Ca^{2+} damaged cell membranes and disrupted electrolytes (GhavamiNejad et al., 2020). Interestingly, based on the direct contact tests and the tests on extracts, F1, F2, and F3 scaffolds were not cytotoxic *in vitro*. However, the RGR of cells treated with the F3 extract was significantly lower than that of the cells treated with the culture media, F1, and F2 extracts. This shows that 80 mM $CaCl_2$ may have had a slight negative impact on the fibroblasts but was not sufficient to induce cytotoxicity in the cell culture environment. For the culture experiments, in the medium extracted from the F1 and F2 scaffolds, there were no significant differences in RGR, compared to the cell culture medium. This suggests that 60 mM and 70 mM concentrations of $CaCl_2$ may be safe for fibroblasts after 24 h of treatment. Furthermore, $CaCl_2$ at a concentration of 100 mM has also been widely used as a crosslinker in other studies, and it has been demonstrated to be non-cytotoxic to cells (GhavamiNejad et al., 2020; Piras and Smith, 2020). In addition, numerous publications have also shown that alginate and gelatin are biocompatible and non-cytotoxic materials (Bose et al., 2018; You et al., 2017). Somasekharan et al. (2020) revealed similar findings, demonstrating that bioinks produced from alginate dialdehyde, gelatin, and PRP are not harmful using tests on extracts (MTT), with cell survival approaching 100% (Somasekharan et al., 2020). These findings inspired us to develop cell–laden bioinks based on gelatin-alginate inks and fabricate printed cell-laden scaffolds. After 24 h of culture, cell viability in these printed scaffolds was determined using the MTT staining technique. The results revealed that the human fibroblasts were still alive and well, producing purple formazan crystals. This demonstrates

that the cells were viable in F1, F2, and F3 scaffolds after being incubated in culture conditions for 24 h. Oxygen and nutrients can be delivered from the surrounding environment to the gelatin-alginate scaffolds. In future studies, we will investigate cell visibility over a more extended period to determine how long cells can proliferate in these printed scaffolds. In addition, the distribution of cells in these printed scaffolds and other scaffold features, such as degradation and swelling ratio, will be investigated in future studies.

5. CONCLUSION

In this study, we designed and fabricated scaffolds from gelatin, alginate, and $CaCl_2$ using 3D extrusion bioprinting. The scaffolds with the $CaCl_2$ crosslinker showed a change in stiffness, compared to the uncrosslinked scaffolds, and the F3 scaffold has the highest rigidity out of the three scaffolds. Additionally, none of the three scaffolds were harmful to human fibroblasts as confirmed by the cytotoxicity tests. Furthermore, human fibroblasts, still survived in the scaffolds made from cell-laden bioinks after 24 h. The results demonstrated that the fabrication of 3D-printed scaffolds can be a potential candidate for future research and development.

ACKNOWLEDGMENT

This research is funded by the University of Science, Ho Chi Minh City, Vietnam, under grant number T2022-24. Additionally, we would like to thank Vietnam National University, Ho Chi Minh City (VNU-HCM), for the partial funding of this study under grant number B2023-18-09.

REFERENCES

Afewerki, S., Sheikhi, A., Kannan, S., Ahadian, S., and Khademhosseini, A. (2019). Gelatin-polysaccharide composite scaffolds for 3D cell culture and tissue engineering: Towards natural therapeutics. *Bioengineering & Translational Medicine,* 4(1), 96−115.

Alizadeh-Osgouei, M., Li, Y., and Wen, C. (2019). A comprehensive review of biodegradable synthetic polymer-ceramic composites and their manufacture for biomedical applications. *Bioactive Materials,* 4, 22−36.

An, J., Teoh, J. E. M., Suntornnond, R., and Chua, C. K. (2015). Design and 3D printing of scaffolds and tissues. *Engineering,* 1(2), 261−268.

Benwood, C., Chrenek, J., Kirsch, R. L., Masri, N. Z., Richards, H., Teetzen, K., and Willerth, S. M. (2021). Natural biomaterials and their use as bioinks for printing tissues. *Bioengineering,* 8(2), 27.

Bose, S., Ke, D., Sahasrabudhe, H., and Bandyopadhyay, A. (2018). Additive manufacturing of biomaterials. *Progress in Materials Science,* 93, 45−111.

Daemi, H., and Barikani, M. (2012). Synthesis and characterization of calcium alginate nanoparticles, sodium homopolymannuronate salt and its calcium nanoparticles. *Scientia Iranica,* 19(6), 2023−2028.

Datta, S., Barua, R., and Das, J. (2020). Importance of alginate bioink for 3D bioprinting in tissue engineering and regenerative medicine. In *Alginates-Recent Uses of This Natural Polymer* (Pereira, L., Cotas, J., Blumenberg, M., Eds.), pp. 1−11. London: IntechOpen.

Fernandes, R. d. S., de Moura, M. R., Glenn, G. M., and Aouada, F. A. (2018). Thermal, microstructural, and spectroscopic analysis of Ca^{2+} alginate/clay nanocomposite hydrogel beads. *Journal of Molecular Liquids,* 265, 327−336.

GhavamiNejad, A., Ashammakhi, N., Wu, X. Y., and Khademhosseini, A. (2020). Crosslinking strategies for 3D bioprinting of polymeric hydrogels. *Small,* 16(35), 2002931.

Giuseppe, M. D., Law, N., Webb, B., Macrae, R. A., Liew, L. J., Sercombe, T. B., Dilley, R. J., and Doyle, B. J. (2018). Mechanical behaviour of alginate-gelatin hydrogels for 3D bioprinting. *Journal of The Mechanical Behavior of Biomedical Materials,* 79, 150−157.

Gopinathan, J., and Noh, I. (2018). Recent trends in bioinks for 3D printing. *Biomaterials Research,* 22(11), 1−15.

Haider, A., Waseem, A., Karpukhina, N., and Mohsin, S. (2020). Strontium-and zinc-containing bioactive glass and alginates scaffolds. *Bioengineering,* 7(1), 10.

Thangaraju, P., and Varthya, S. B. (2022). ISO 10993: Biological evaluation of medical devices. In *Medical Device Guidelines and Regulations Handbook* (Shanmugam, P. S. T., Thangaraju, P., Palani, N., and Sampath, T., Eds.), (pp. 163-187). Cham: Springer.

Klouda, L., and Mikos, A. G. (2008). Thermoresponsive hydrogels in biomedical applications. *European Journal of Pharmaceutics and Biopharmaceutics,* 68(1), 34−45.

Nelson, C., Tuladhar, S., Launen, L., and Habib, A. (2021). 3D bio-printability of hybrid pre-crosslinked hydrogels. *International Journal of Molecular Sciences,* 22(24), 13481.

Pan, T., Song, W., Cao, X., and Wang, Y. (2016). 3D bioplotting of gelatin/alginate scaffolds for tissue engineering: Influence of crosslinking degree and pore architecture on physicochemical properties. *Journal of Materials Science & Technology,* 32(9), 889−900.

Piras, C. C., and Smith, D. K. (2020). Multicomponent polysaccharide alginate-based bioinks. *Journal of Materials Chemistry B,* 8(36), 8171−8188.

Ramiah, P., du Toit, L. C., Choonara, Y. E., Kondiah, P. P., and Pillay, V. (2020). Hydrogel-based bioinks for 3D bioprinting in tissue regeneration. *Frontiers in Materials,* 7, 76.

Roi, A., Ardelean, L. C., Roi, C. I., Boia, E.-R., Boia, S., and Rusu, L.-C. (2019). Oral bone tissue engineering: Advanced biomaterials for cell adhesion, proliferation and differentiation. *Materials,* 12(14), 2296.

Rottensteiner, U., Sarker, B., Heusinger, D., Dafinova, D., Rath, S. N., Beier, J. P., Kneser, U., Horch, R. E., Detsch, R., Boccaccini, A. R., and Arkudas, A. (2014). *In vitro* and *in vivo* biocompatibility of alginate dialdehyde/gelatin hydrogels with and without nanoscaled bioactive glass for bone tissue engineering applications. *Materials,* 7(3), 1957−1974.

Sahoo, D. R., and Biswal, T. (2021). Alginate and its application to tissue engineering. *SN Applied Sciences,* 3(1), 30.

Somasekharan, L., Kasoju, N., Raju, R., and Bhatt, A. (2020). Formulation and characterization of alginate dialdehyde, gelatin, and platelet-rich plasma-based bioink for bioprinting applications. *Bioengineering,* 7(3), 108.

Tan, J. J. Y., Lee, C. P., and Hashimoto, M. (2020). Preheating of gelatin improves its printability with transglutaminase in direct ink writing 3D printing. *International Journal of Bioprinting,* 6(4), 296.

Unagolla, J. M., and Jayasuriya, A. C. (2020). Hydrogel-based 3D bioprinting: A comprehensive review on cell-laden hydrogels, bioink formulations, and future perspectives. *Applied Materials Today,* 18, 100479.

Vitus, V., Ibrahim, F., and Zaman, W. S. W. K. (2021). Modelling of stem cells microenvironment using carbon-based scaffold for tissue engineering application–A review. *Polymers,* 13(23), 4058.

You, F., Wu, X., and Chen, X. (2017). 3D printing of porous alginate/gelatin hydrogel scaffolds and their mechanical property characterization. *International Journal of Polymeric Materials and Polymeric Biomaterials,* 66(6), 299–306.

Zhang, X., Wang, X., Fan, W., Liu, Y., Wang, Q., and Weng, L. (2022). Fabrication, property and application of calcium alginate fiber: A review. *Polymers,* 14(15), 3227.